Progress in Nuclear Energy 57 (2012) 77–85

Contents lists available at SciVerse ScienceDirect

Progress in Nuclear Energy

journal homepage: www.elsevier.com/locate/pnucene

In situ TEM observation of interactions between gliding dislocations and prismatic loops in Zr-ion irradiated zirconium alloys

F. Onimus [a,*], L. Dupuy [a], F. Mompiou [b]

[a] SRMA-CEA, CEA-Saclay, 91191 Gif-Sur-Yvette, France
[b] CEMES-CNRS, BP 4347, 31055 Toulouse, France

ARTICLE INFO

Article history:
Received 11 August 2011
Accepted 6 September 2011

Keywords:
Zirconium
Irradiation
Dislocation
Loop
Junction
In situ
Transmission electron microscopy

ABSTRACT

Zirconium alloys cladding tubes containing the fuel of pressurized water nuclear reactors constitute the first barrier against the dissemination of radioactive elements. It is therefore essential to have a good understanding of the effects of neutron radiation on the deformation mechanisms of these materials. In order to study the effect of irradiation on the deformation mechanisms, zirconium alloys specimens have been irradiated with Zr ions at 350 °C and 500 °C. On these specimens in situ TEM tensile tests have been carried out at 350 °C and the interactions between gliding dislocations and radiation induced loops have been observed. It has been shown that in the case of edge dislocations gliding in prismatic planes, the loops can be incorporated within the dislocation as super-jog explaining the clearing of loops by gliding dislocations. However, it has also been shown that in specific configuration, the dislocation gliding in prismatic plane is strongly pinned by the loop, explaining the difficult activation of prismatic slip after irradiation resulting in the strong radiation induced hardening.

1. Introduction

Nuclear reactor components made from zirconium alloys, such as cladding tubes containing the fuel of nuclear reactor, undergo fast neutron damage. This neutron damage induces major changes on microscopic deformation mechanisms. In order to understand and, in a future prospect, to predict the macroscopic mechanical behaviour of irradiated Zr alloys, it is essential to have a thorough experimental analysis of the microscopic deformation mechanisms.

It is known that in zirconium alloys, radiation damage consists mainly in the formation of small prismatic loops with <a> Burgers vector type lying on {10$\bar{1}$0} prismatic habit planes (Northwood, 1977; Jostsons et al., 1977; Northwood et al., 1979; Griffiths, 1988; Onimus & Béchade, in press). The <a> loops are found to be of either vacancy or interstitial type with <a> Burgers vector. The three loop populations (three <a> Burgers vectors are possible in the hexagonal closed packed structure) are found in the same proportion (Kelly and Blake, 1973). Furthermore, these <a> loops are perfect and therefore glissile on their cylinder.

As reviewed in (Hirsch, 1976; Was, 2007), the increase in strength observed in irradiated metals is attributed to the presence of the high density of these small radiation-induced loops that act as obstacles against dislocation glide. Indeed, according to (Hirsch, 1976; Foreman and Sharp, 1969; Saada and Washburn, 1962) when a gliding dislocation encounters a loop, a junction can be created and constitute a pining point for the gliding dislocation. Nevertheless, the dislocation can drag or annihilate the loop following various possible mechanisms as described in (Hirsch, 1976; Foreman and Sharp, 1969; Saada and Washburn, 1962; Strudel and Washburn, 1964; Wechsler, 1973) in the case of Face Centred Cubic (FCC) metals. The removal of irradiation loops by moving dislocations produces a defect-free channel that constitutes a preferred area for further dislocation gliding leading to the channelling of the dislocations as discussed in (Wechsler, 1973; Sharp, 1967, 1972; Makin, 1970; Luft, 1991). Dislocation channelling has been observed in various irradiated metals as reviewed in (Wechsler, 1973).

In the case of zirconium alloys, several authors have observed defect free channels in a Transmission Electron Microscope (TEM) (Coleman et al., 1972; Williams et al., 1974; Onchi et al., 1980; Pettersson, 1982; Adamson and Bell, 1985; Fregonese et al., 2000; Régnard et al., 2002). Although the easy glide slip system is the prismatic system at 350 °C before irradiation (Onimus et al., 2004, 2005), the basal slip becomes the easy slip system after irradiation (at 350 °C). This change of the easy glide slip system has been attributed (Onimus et al., 2004, 2005) to the difference in interactions between radiation induced loops and dislocations gliding either in the basal plane or in the prismatic plane. Carpenter

* Corresponding author.
E-mail address: fabien.onimus@cea.fr (F. Onimus).

0149-1970/$ – see front matter © 2011 Elsevier Ltd. All rights reserved.
doi:10.1016/j.pnucene.2011.10.005

Table 1
Chemical composition (wt%) of the recrystallized Zircaloy-4.

Alloy	Sn	Fe	Cr	O	Zr
Zy-4	1.30	0.210	0.100	0.125	bal.

(Carpenter, 1976) has also investigated theoretically, in specific cases, the junction reaction between loops and gliding dislocations. More recently, molecular dynamic calculations (Voskoboynikov et al., 2005a,b) have been used in order to investigate details of dislocation–loop interactions in specific cases for irradiated Zr alloys. However, the main differences between prismatic and basal slip are not yet clearly understood.

In order to have a better understanding of the origin of the dislocation channelling mechanism and the change of the easy slip system after irradiation, recrystallized Zircaloy-4 specimens have been irradiated with Zr-ion. After irradiation, the specimens have been tested under uniaxial tensile strain in situ in a TEM, allowing the direct observation of the interaction between gliding dislocations and radiation induced loops.

2. Materials and experimental details

A Zircaloy-4 recrystallized thin sheet of 0.4 mm thickness was used for this experiment. The chemical composition of the material is given in Table 1. A 120 μm × 90 μm Electron Back Scattering Diffraction (EBSD) map of the sheet in the Rolling Direction (RD) - Transverse Direction (TD) plane is given in Fig. 1. The measured mean grain size is 5 μm. The {0001} pole figure determined by EBSD is given in Fig. 2. Note that the texture of the sheet exhibits a high density of {0001} poles close to the normal of the sheet.

Small samples, 5.5 mm long and 1.8 mm wide, were machined out in the RD-TD plane with their longest dimension oriented along the transverse direction of the rolled sheet. Two holes of 0.4 mm diameter were also machined at both ends of the specimens in order to be able to grip the specimen in the testing holder. The samples were then grinded down to a thickness of 0.1 mm and then electropolished on one side in order to create a dimple in the centre. The irradiation was performed at 350 °C and 500 °C at various doses on the polished side of the samples

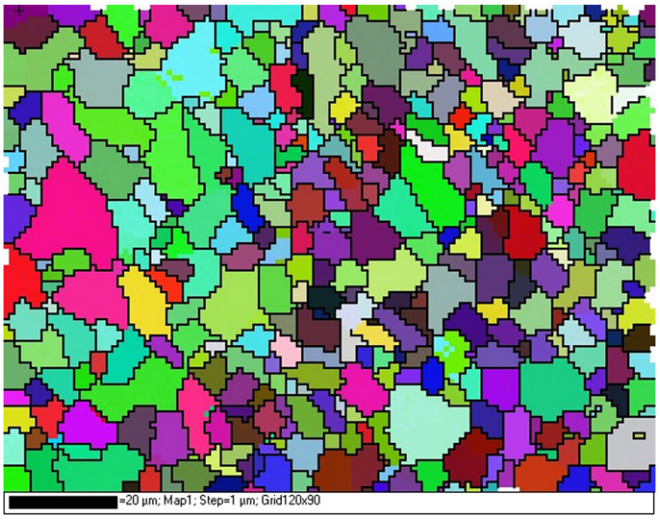

Fig. 1. Orientation map of the grains in the RD-TD plane obtained by Electron Back Scattering Diffraction (EBSD). Euler angle-based color scale is used here.

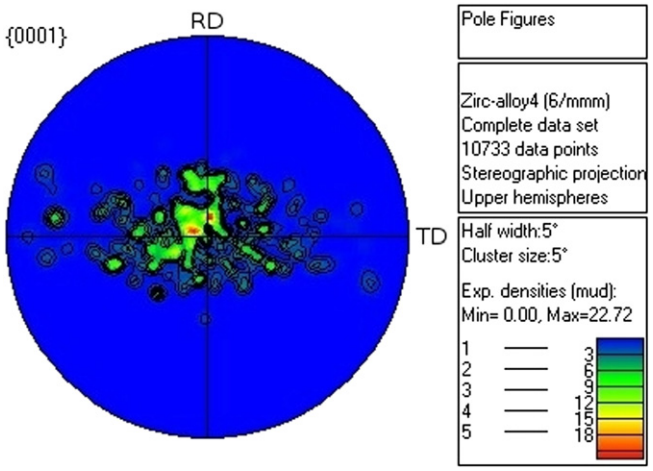

Fig. 2. {0001} pole figures obtained by Electron Back Scattering Diffraction on the RD-TD plane.

using Zr ions at CSNSM/IN2P3 in Orsay on the TANDEM accelerator ARAMIS facility (Bernas et al., 1992; Cottereau et al., 1990). A special sample holder was designed in order to maintain the specimens during the Zr-ion irradiation. Two energies for the Zr ions were used in order to obtain a relatively flat damage profile in the thin foil. The energies and doses for these two irradiations are given in Table 2. The SRIM simulation of the damage profile for both irradiations are shown in Figs. 3 and 4 using $E_d = 40$ eV as displacement energy for zirconium. The mean damage in the thickness of the thin foil, taken as 150 μm thick, is also given in Table 2. After irradiation, the specimen surface was protected thanks to a varnish and the other side was electropolished until the formation of an electron transparent hole. The varnish was then removed. The observed area of the thin foil which was about 150 nm thick, was therefore fully irradiated.

The irradiated specimens were then introduced into a special TEM sample holder for in situ tensile testing experiment as presented in (Verhaeghe et al., 1997; Ambard et al., 2001). In this holder the specimen can be rotated along the straining axis about ±30° (primary tilt). A small secondary tilt of ±5° with a rotation axis perpendicular to the primary one is also allowed in order to obtain correct two beams diffraction conditions. The holder is also equipped with a furnace which allows the heating of the sample at a temperature of 350 °C. The temperature is measured by a thermocouple with an accuracy of 5 °C. Experiments were carried out in a JEOL 3010 operated at 300 kV. A force was first progressively applied, and when dislocation motion was observed, the load was maintained constant and dislocation motion was recorded by a CCD camera. Images were then extracted from video sequences in order to illustrate the observed mechanisms. *Post-mortem* analysis of slip traces and grain orientation were also performed using single tilt sample holder after testing.

3. Results

3.1. As-irradiated microstructure

Before testing, the loop microstructure has been observed and characterized by TEM. The irradiation induced microstructure consists of prismatic dislocation loops with <a> Burgers vector. The loop density and the diameter of loops have been estimated for the two irradiation conditions (taking into account an estimated thickness of 150 nm for the thin foil) (Table 3). The diameter of the

Table 2
Irradiation conditions.

Specimens	Energy	Flux (ions.cm^{-2}.s^{-1})	Dose (ions.cm^{-2})	Mean damage in the thin foil (dpa)	Mean damage rate i n the thin foil (dpa.s^{-1})	Irradiation Temperature
A	1 MeV	6.7×10^{10}	20×10^{13}	1.3	3×10^{-4}	350 °C
	0.6 MeV	5.1×10^{10}	5×10^{13}			
B	2 MeV	7.7×10^{10}	5×10^{13}	0.3	3×10^{-4}	500 °C
	0.6 MeV	5.2×10^{10}	1.5×10^{13}			

largest loops observed is also given in Table 3, illustrating the size distribution of loops for each irradiation condition. These results are in correct agreement with the TEM observations performed by Hellio et al. (Hellio et al., 1988) on Zr-ion irradiated Zircaloy-4 at 450 °C up to 0.7 dpa, where loops exhibit a mean diameter of 7 nm and a density of 26×10^{21} m^{-3}.

3.2. In situ observations of dislocation motion in the unirradiated material

First, unirradiated specimens have been tested at 350 °C. As the load is increased, dislocations segments started to move in the grains situated on the lateral side of the hole with respect to the applied force direction, where the stress is maximum and the first principal stress direction parallel to the straining direction (Coujou et al., 1990). Dislocations seemed to be emitted from grain boundaries situated away from the hole in thicker areas. At low applied loads, very slow dislocation motions were recorded and few grains exhibited slip traces. At higher applied load, faster dislocation motions were recorded, and all the grains in the deformed area exhibited slip traces (Fig. 5). According to Hirsch (Hirsch, 1965) these slip traces are due to the strain field left by the dislocation in the oxide layers at both surfaces. They exhibit therefore a broad contrast which obey the same extinction rules than the dislocations which have just glided. After in situ testing, the slip traces were analyzed. They systematically correspond to prismatic slip plane in agreement with the in situ tensile tests performed by Farenc et al. (Farenc et al., 1993) in titanium. Due to the strong texture of the material, the dislocations which have glided in the primatic plane in the thin foil were mainly of edge character and their slip traces are along the <a> direction.

3.3. In situ observations of loop clearing in specimens irradiated at 350 °C

Fig. 6 shows an edge dislocation moving in a prismatic plane in a specimen irradiated at 350 °C (referred as A specimens in Table 2). The dislocation position is indicated by white arrows. For the sake of clarity, the dislocation initial position and slip traces have been drawn. It can be clearly seen that the contrast which is initially dark and blurred due to the strain field of numerous small radiation induced loops, becomes white and clear in the wake of the dislocation. This indicates that the induced irradiation loops are progressively cleared. Numerous thin slip bands cleared of defects were observed after testing in the whole specimen as shown in Fig. 7. The slip traces analysis shows that only prismatic glide has occurred during the test. Due to the strong texture of the rolled sheet, the grain orientation is such that the <c> direction is close to the normal to the thin foil. Therefore, the gliding dislocations are essentially edge character proving that edge <a> dislocations gliding in the prismatic plane are able to clear the <a> loops. At high magnification, it can be seen that many loops are still present inside the cleared traces showing that these traces were only partly cleared by gliding dislocations.

3.4. In situ observations of interaction between dislocation and loop in the specimens irradiated at 500 °C

Due to the high loop density in the specimens A (irradiated at 350 °C), the in-situ observation of a single dislocation-loop interaction is hardly possible. In order to have a better understanding of

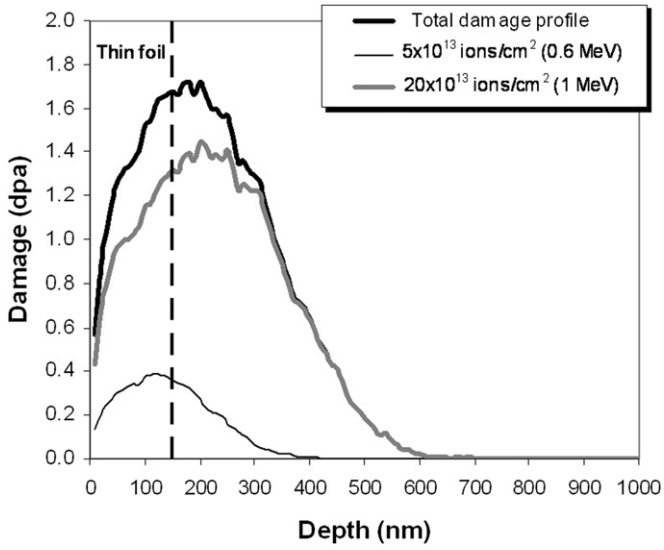

Fig. 3. SRIM damage profile obtained for 5×10^{13} ions/cm^2 Zr ions with energy 0.6 MeV and 20×10^{13} ions/cm^2 Zr ions with energy 1 MeV in a target made of Zr. A displacement energy of $E_d = 40$ eV is used. The total damage profile is also given.

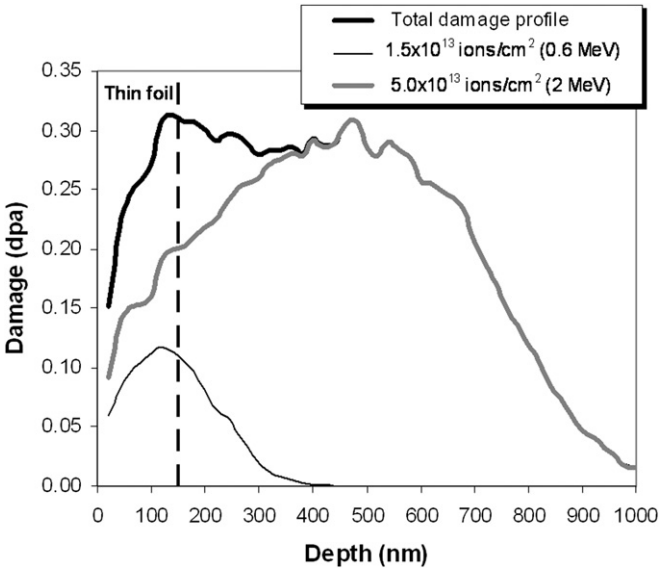

Fig. 4. SRIM damage profile obtained for 1.5×10^{13} ions/cm^2 Zr ions with energy 0.6 MeV and 5×10^{13} ions/cm^2 Zr ions with energy 1 MeV in a target made of Zr. A displacement energy of $E_d = 40$ eV is used. The total damage profile is also given.

Table 3
Loop density and mean diameter of loops for the two irradiation conditions. The diameter of the largest loops observed is also given.

Specimens	Irradiation Temperature	Mean damage in the thin foil (dpa)	Mean diameter (nm)	Diameter of the largest loops observed (nm)	Loop density[a] (m^{-3})
A	350 °C	1.3	3	9	$\sim 50 \times 10^{21}$
B	500 °C	0.3	12	42	$\sim 5 \times 10^{21}$

[a] The thickness of the thin foil is estimated as 150 nm.

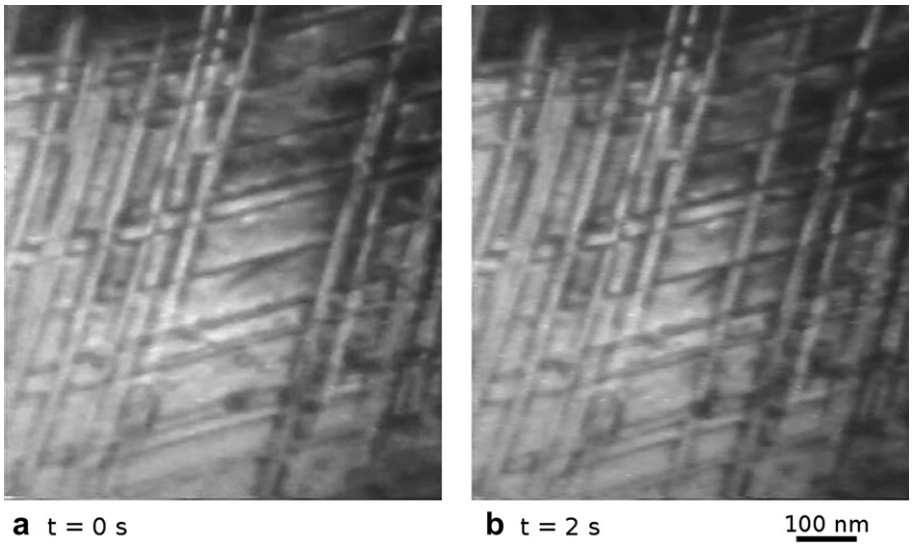

Fig. 5. In situ observation of the formation of slip traces, corresponding to the prismatic slip plane, by the glide of edge dislocation segment in the thin foil made of recrystallized Zircaloy-4.

the detailed clearing mechanism, similar experiments were carried out in samples with a lower loop density and larger loop size (referred as specimens B in Table 2). During the experiment various interactions mechanisms were observed. Fig. 8 shows a loop annihilated by an edge dislocation gliding in the prismatic plane. On the contrary, the loop can act as a strong pinning point for the

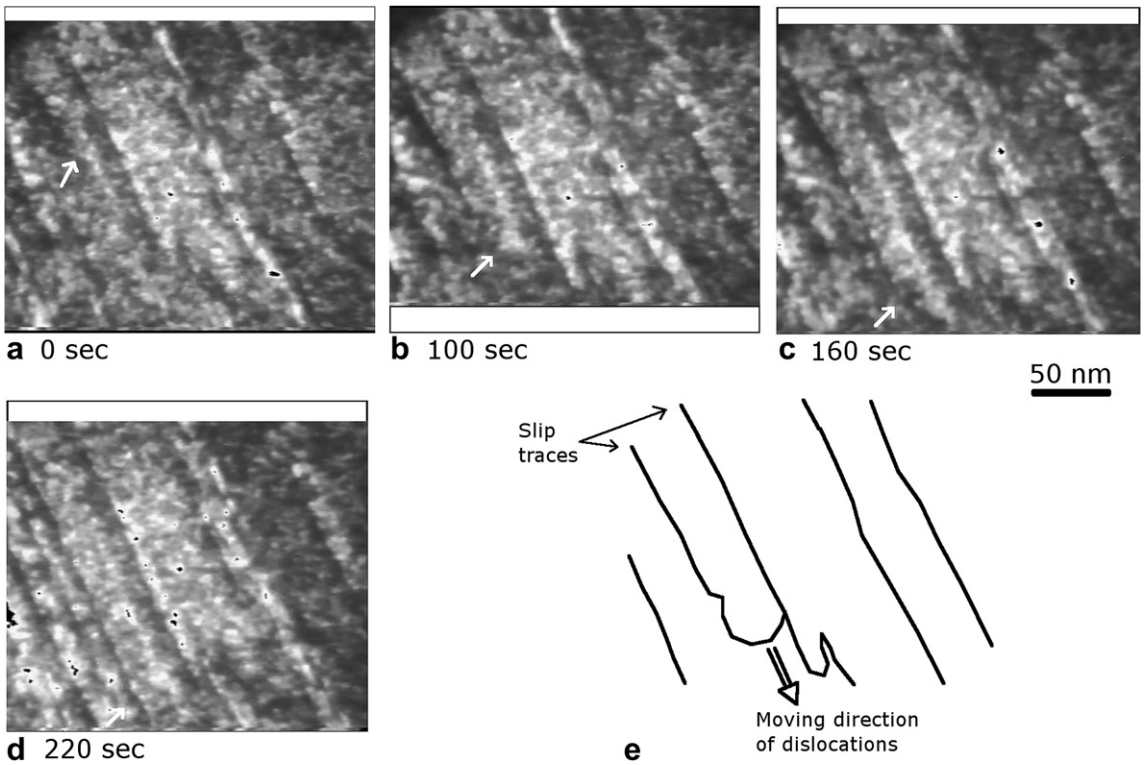

Fig. 6. In situ observation of the formation of cleared bands, by clearing of loops by edge dislocation gliding in the prismatic slip plane in Zr-ion irradiated recrystallized Zircaloy-4. The arrows point on different position of the dislocation at different times during its motion. The dislocation and slip traces are drawn for clarity in (e).

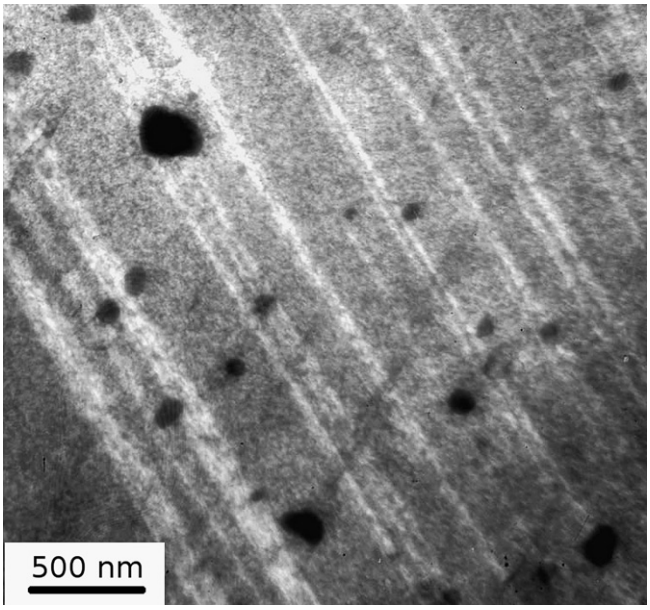

Fig. 7. Cleared bands observed after in-situ testing at 350 °C in specimens made of recrystallized Zircaloy-4 irradiated up to 1.3 dpa at 350 °C with Zr-ion.

edge dislocation gliding in the prismatic plane as shown in Fig. 9. Indeed in this case, it can be seen that the moving dislocation bend around the loop.

The analysis of the slip traces indicates that the dislocations have glided in the prismatic plane and are elongated along their screw parts (Fig. 10) (the <a> direction). Note in Fig. 10 that the slip traces and the dislocations, are much more wavy than in the unirradiated material (Fig. 5).

4. Discussion

The observation of the clearing of loops by dislocations gliding in the prismatic plane is consistent with the formation of prismatic channels during axial tensile tests, when the basal plane is not well orientated for slip, at 350 °C on recrystallized zirconium alloys cladding tube irradiated with neutron, as reported in (Onimus et al., 2004). However, in (Onimus et al., 2004) it has also been proven that the easy glide slip system at 350 °C after irradiation is the basal slip system, the clearing of loops being easy along the basal planes and more difficult along the prismatic planes. In this present work, only prismatic glide is observed, no basal glide is seen.

This difference can be first attributed to the strong texture of the thin sheet that exhibits a high density of {0001} poles along the Normal Direction of the sheet. Indeed, in the case of this material, for tensile tests performed in the Rolling Direction as well as in the Transverse Direction, the Schmid factors of the basal slip systems are very low. The basal slip is therefore not likely to be activated. On the other hand, in the study described in (Onimus et al., 2004) the materials were cladding or thick sheets that exhibit texture with {0001} poles tilted in the ND-TD plane. This explains why basal channels were more easily observed for these materials.

Another reason for the difference in mechanisms observed in situ compared to tests performed on bulk material, is the effect of the thin foil associated with the orientation of the grains. Indeed, in the case of bulk material, the dislocations sources, like Frank-Read sources, emit dislocations that glide throughout the 5 μm diameter equiaxed grains allowing complex 3D motion within the grain such as cross-slip for the screw part of the dislocations. On the other hand, in the case of these thin foils, only short edge dislocation segments glide in the thin foil which is about 150 nm thick. The creation of the observed cleared bands is therefore believed to be very different on thin foil than on bulk material where broadening of the channel by cross-slip can occur. Nevertheless, single

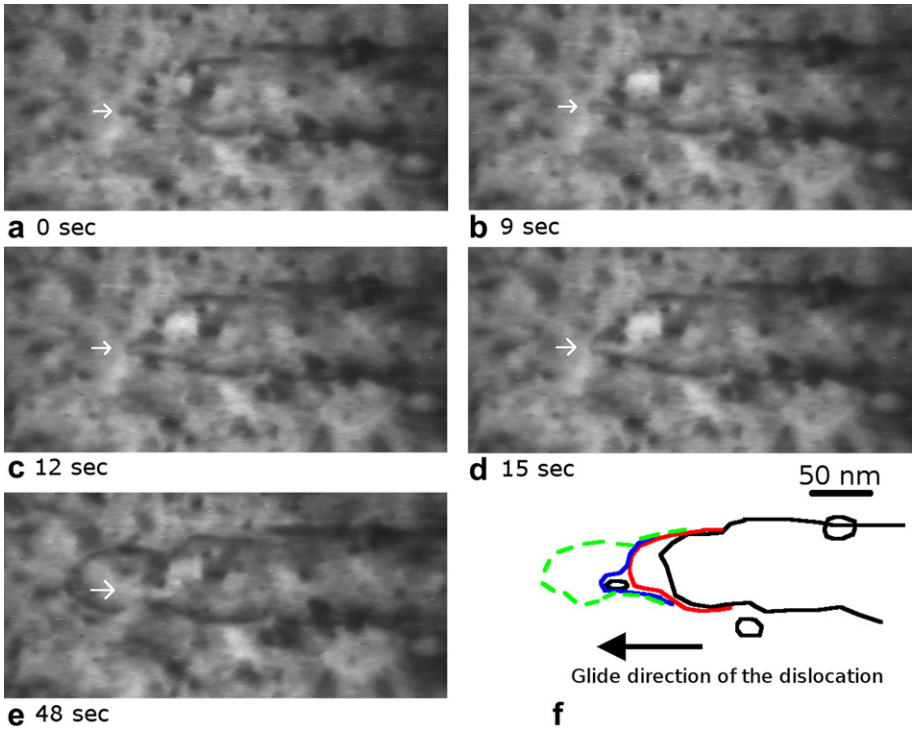

Fig. 8. In situ observation at 350 °C, on Zr-ion irradiated Zircaloy-4, of the incorporation of a loop into an edge dislocation gliding in the prismatic plane. The white arrows indicate the position of the loop. The different dislocation positions are drawn in (f).

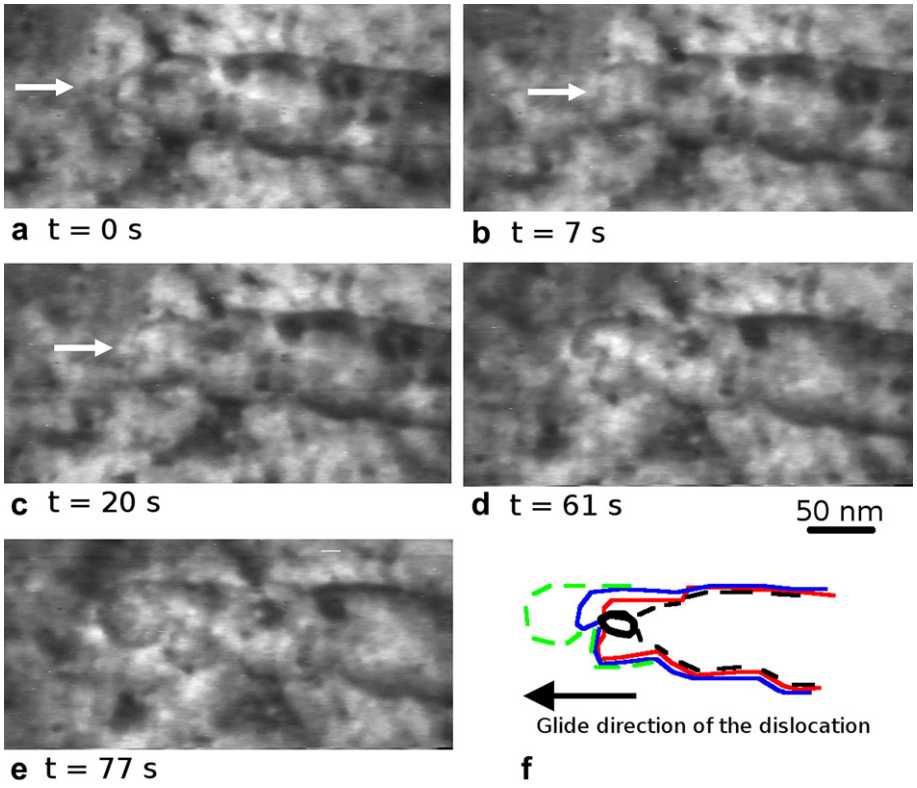

Fig. 9. In situ observation at 350 °C, on Zr-ion irradiated Zircaloy-4, of the strong pinning by a loop of an edge dislocation gliding in the prismatic plane. The white arrows indicate the position of the loop. The different dislocation positions are drawn in (f).

interaction between gliding dislocation and loops can be accurately studied using this technique.

The observation of the clearing of one loop by an edge dislocation gliding in the prismatic plane, reported in Fig. 8, can be easily understood when the Burgers vector of the loop and the Burgers vector of the gliding dislocation are the same.

Indeed, according to (Saada and Washburn, 1962), if the loop has the same or opposite Burgers vector as the edge gliding dislocation (e.g. $\underline{b}_G = \underline{a}_1$ and $\underline{b}_L = -\underline{a}_1$ where $\underline{b}_G$ and $\underline{b}_L$ respectively stand for the Burgers vectors of gliding dislocation and loop), one part of the loop is incorporated into the dislocation (Fig. 11). Here, the Burgers vectors and the line directions are chosen such that the sum of the Burgers vectors at each node is equal to zero. This mechanism creates a super-jog on the dislocation. This super-jog can either be above or below the glide plane of the dislocation depending on the nature of the loop and the Burgers vector of the edge dislocation. The sweeping of the jog on its cylinder is possible leading to the progressive destruction of the radiation induced loops by gliding dislocations, as suggested in (Veyssière, 2001), therefore explaining the creation of the cleared bands observed in Fig. 7.

It is also worth noting that in Fig. 8, the loop is not attracted by the dislocation although the loop is perfect and can therefore glide on its cylinder. This is probably the result of the trapping of solute atoms, such as oxygen, by the loop which decreases its mobility on its cylinder.

Wavy slip traces have been observed after testing in Fig. 10. It is likely that these so-called "slip traces" are in fact wavy dislocations trapped below the surface oxide layer. Indeed, such wavy slip traces are not expected on the surface of the specimen if we assume that the surface is flat. More they do not exhibit the typical broad contrast of slip traces as shown in Fig. 5. The observation of these wavy dislocations orientated along the screw direction of the dislocation (the <a> direction) can be understood by considering that edge segments moving in the prismatic plane trail increasingly long screw segments blocked below the surface. These screw segments can incorporate irradiation loops. Indeed, according to

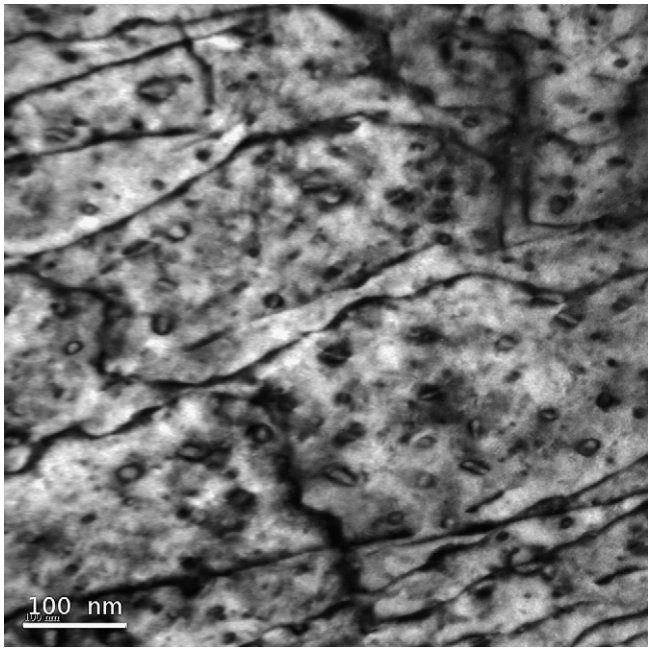

Fig. 10. Wavy slip traces, or dislocations, observed after in situ testing at 350 °C on Zr-ion irradiated Zircaloy-4.

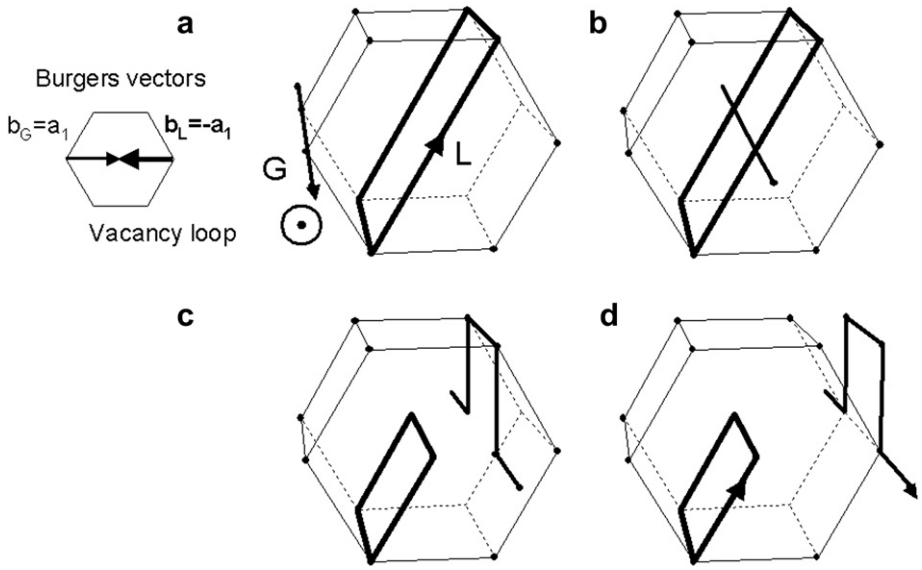

Fig. 11. Schematic describing the incorporation of a part of the loop as a super-jog into the edge dislocation gliding in the prismatic plane. L stands for loop and G for gliding dislocation. Vacancy loop is shown here.

(Strudel and Washburn, 1964) when the loop has the same, or opposite, Burgers vector as the screw dislocation, the loop is incorporated into the screw dislocation leading to the creation of a helical super-jog, or helix turn (Fig. 12). The orientation of this helical jog depends on the relative Burgers vector of the dislocation and the nature of the loop. On a purely screw dislocation this super-jog is a strong pinning point since it can only glide on its cylinder along the dislocation line. Pure screw dislocations are therefore believed to be strongly impeded by loops. This is believed to lead to a strong discrepancy in the mobility between edge and screw dislocations, as pointed out in (Nogaret et al., 2007, 2008). However, in the case of a mixed dislocation, the helical super-jog can be pushed aside, on its glide cylinder.

The configuration observed in Fig. 9, when the loop acts as a strong pinning point for dislocation glide, can be explained by considering that the edge dislocation gliding in the prismatic plane and the loop have different Burgers vectors (e.g. $\underline{b}_G = \underline{a}_1$ and $\underline{b}_L = \underline{a}_3$). In that case, an attractive junction can be formed (Hirsch, 1976; Foreman and Sharp, 1969; Saada and Washburn, 1962). Since both the gliding dislocation and the loop have a <a> type Burgers vector the Burgers vector of the created junction possesses the third <a> type Burgers vector ($\underline{b}_J = \underline{a}_2$). The junction is therefore not able to glide in the prismatic plane of the gliding dislocation. This junction is therefore sessile and acts as a strong pinning point for the gliding dislocation. Nevertheless, for high applied stress this pinning point can be overcome, for instance via the mechanism proposed in Fig. 13. For this proposed mechanism, the gliding dislocation pulls the junctions so that the loop progressively flips into the gliding plane of the dislocation. Eventually the dislocation overcomes the loop, leaving the loop behind with a modified habit

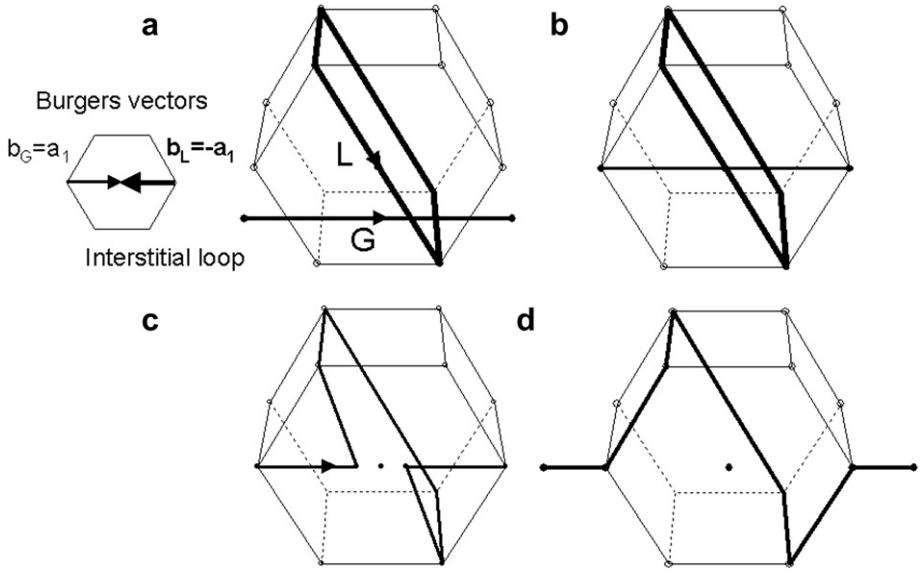

Fig. 12. Schematic describing the incorporation of a loop as a super-jog into a screw dislocation gliding in the prismatic plane. L stands for loop and G for gliding dislocation. Interstitial loop is shown here.

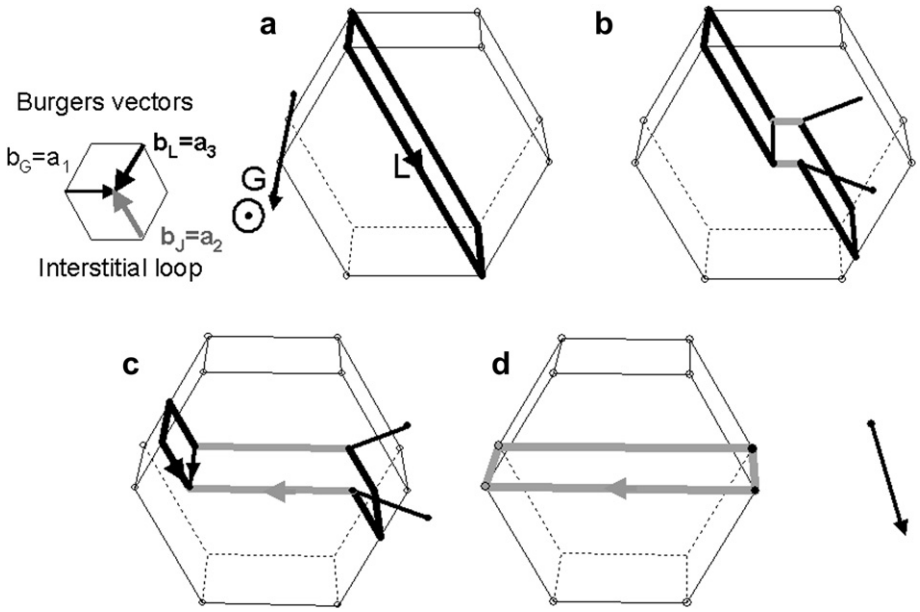

Fig. 13. Schematic describing junctions formation between a loop and an edge dislocation gliding in the prismatic plane with different Burgers vectors. L stands for loop, G for gliding dislocation and J for junction. Interstitial loop is shown here.

plane and modified Burgers vector. More accurate dislocation dynamic computations are required to assess the detailed interactions between dislocation and loop.

On the other hand when the dislocation, either screw or edge, gliding in the basal plane interacts with a loop with different Burgers vectors, attractive junctions are formed. As in the previous case, the Burgers vector of the created junction possesses the third <a> type Burgers vector (e.g. $\underline{b}_J = \underline{a}_2$) as shown in Fig. 14. Since all three <a> type Burgers vectors belong to the basal plane, the junction is able to glide in the basal plane like the dislocation. The loop can therefore be swept aside by the dislocation on its glide cylinder, the junction also gliding in the basal plane. This can explain why the basal channelling is favoured after irradiation whereas the prismatic channelling is more difficult.

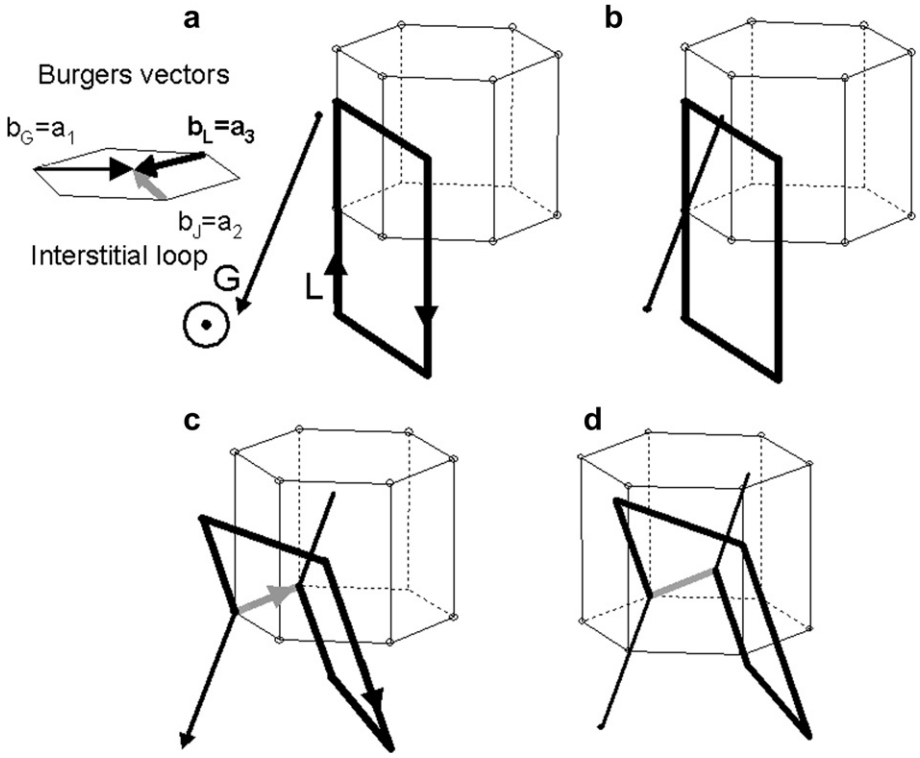

Fig. 14. Schematic describing junctions formation between a loop and an edge dislocation gliding in the basal plane with different Burgers vectors. L stands for loop, G for gliding dislocation and J for junction. Interstitial loop is shown here.

5. Conclusions

Interactions between radiation induced loops and gliding dislocations have been studied by in-situ TEM tensile test in Zr-ion irradiated recrystallized Zircaloy-4 specimens. It was shown that for a high density of loops, dislocations gliding in the prismatic planes can erase irradiation loops along thin channels. Moreover, when the loops are larger and in lower density, the incorporation of one loop into an edge dislocation gliding in the prismatic plane has been observed. This explains the clearing of loops as well as the observation of prismatic channels, in specific case, in neutron irradiated zirconium alloys. In another configuration, it has been observed that a loop acts as strong pinning point for an edge dislocation gliding in the prismatic plane, explaining the strong radiation induced hardening observed at macroscopic scale. A detailed theoretical analysis of the junction formation between dislocation and loops show that when a junction is formed between a loop and a dislocation gliding in the prismatic plane, the junction is sessile whereas when the dislocation glides in the basal plane, the junction is glissile, therefore explaining the easier basal channelling observed in neutron irradiated zirconium alloys. More accurate dislocation dynamic computations, that have recently been undertaken, are nevertheless required to assess more precisely the detailed interactions between dislocations and loops in irradiated zirconium alloys.

Acknowledgements

Great acknowledgements are given to Laure Guetaz and Béatrice Doisneau-Cottignies for their help in the in situ testing experiments. The authors also want to thank Malcolm Griffiths for fruitful discussions.

References

Adamson, R.B., Bell, W.L., vol. 1, International Symposiums, Xian, China, pp. 237–246, 1985.
Ambard, A., Guétaz, L., Louchet, F., Guichard, D., 2001. Mater. Sci. Eng. A 319–321, 404–408.
Bernas, H., Chaumont, J., Cottereau, E., Meunier, R., Traverse, A., Clerc, C., Kaitasov, O., Lalu, F., Le Du, D., Moroy, G., Salomé, M., 1992. Nucl. Instruments Methods Phys. Res. Sect. B. Beam Interactions Mater. Atoms 62 (3), 416–420.
Carpenter, G.J.C., 1976. Scripta Metallurgica 10, 411–413.
Coleman, C.E., Mills, D., van der Kuur, J., 1972. Can. Metallurgical Quaterly 11, 91–100.
Cottereau, E., Camplan, J., Chaumont, J., Meunier, R., Bernas, H., 1990. Nucl. Instruments Methods Phys. Res. Sect. B. Beam Interactions Mater. Atoms 45 (1–4, 2), 293–295.
Coujou, A., Lours, Ph., Roy, N.A., Caillard, D., Clément, N., 1990. Acta Metall. Mat. 38, 825.
Farenc, S., Caillard, D., Couret, A., 1993. Acta Metallurgica et Materialia 41 (9), 2701–2709.
Foreman, A.J.E., Sharp, J.V., 1969. Phil. Mag 19, 931.
Fregonese, M., Régnard, C., Rouillon, L., Magnin, T., Lefebvre, F., Lemaignan, C., 2000. Zirconium in Nuclear Industry: Twelfth International Symposium. ASTM STP, 1354, pp. 377–398.
Griffiths, M., 1988. J. Nucl. Mat 159, 190–218.
Hellio, C., de Novion, C.H., Boulanger, L., 1988. J. Nucl. Mater. 159, 368–378.
Hirsch, P.B., 1965. Electron Microscopy of Thin Crystals. Butterworths.
Hirsch, P.B., 1976. Proceedings of a Conference on Point Defect Behavior and Diffusional Processes. University of Bristol.
Jostsons, A., Kelly, P.M., Blake, R.G., 1977. J. Nucl. Mat 66, 236–256.
Kelly, P.M., Blake, R.G., 1973. Phil. Mag 28, 415–426.
Luft, A., 1991. Prog. Mater. Sci. 35, 97–204.
Makin, M.J., 1970. Philos. Mag. 21, 815–821.
Nogaret, T., Robertson, C., Rodney, D., 2007. Phil. Mag. 87 (6), 945–966.
Nogaret, T., Rodney, D., Fivel, M., Robertson, C., 2008. J. Nucl. Mater. 380, 22–29.
Northwood, D.O., Gilbert, R.W., Bahen, L.E., Kelly, P.M., Blake, R.G., Jostsons, A., Madden, P.K., Faulkner, D., Bell, W., Adamson, R.B., 1979. J. Nucl. Mat 79, 379–394.
Northwood, D.O., 1977. At. Energy Rev. 15 (4), 547–610.
Onchi, T., Kayano, H., Higashiguchi, Y., 1980. J. Nucl. Mat 88, 226–235.
Onimus, F., Béchade, J.L., Radiation Effects in Zirconium Alloys, Comprehensive Nuclear Materials, R. Konings Ed., Elsevier Ltd., ISBN: 978-0-08-056027-4, in press.
Onimus, F., Monnet, I., Béchade, J.L., Prioul, C., Pilvin, P., 2004. J. Nucl. Mater. 328, 165–179.
Onimus, F., Béchade, J.L., Prioul, C., Pilvin, P., Monnet, I., Doriot, S., Verhaeghe, B., Gilbon, D., Robert, L., Legras, L., Mardon, J.-P., 2005. J. ASTM Int. 2 (8).
Pettersson, K., 1982. J. Nucl. Mat 105, 341–344.
Régnard, C., Verhaeghe, B., Lefebvre-Joud, F., Lemaignan, C., 2002. Zirconium in the Nuclear Industry, 13th International Symposium. ASTM STP, 1423, pp. 384–399.
Saada, G., Washburn, J., 1962. Proceedings of the international conference on crystal lattice defects. Symp. J. physical society Jpn. 18 Supplement 1, 1963.
Sharp, J.V., 1967. Philos. Mag 16, 77–96.
Sharp, J.V., 1972. Radiat. Effects 14, 71.
Strudel, J.L., Washburn, J., 1964. Pilots. Mag 9, 491–506.
Verhaeghe, B., Louchet, F., Doisneau-Cottignies, B., Bréchet, Y., Massoud, J.-P., 1997. Philos. Mag. A 76 (5), 1079–1091.
Veyssière, P., 2001. Phil. Mag Lett. 81 (11), 733–741.
Voskoboynikov, R.E., Osetsky, Yu. N., Bacon, D.J., 2005a. Mater. Sci. Eng. A 400–401, 54–58.
Voskoboynikov, R.E., Osetsky, Yu. N., Bacon, D.J., 2005b. Mater. Sci. Eng. A 400–401, 49–53.
Was, G.S., 2007. Fundamentals of Radiation Materials Science (Metals and Alloys). Springer Verlag.
Wechsler, M.S., 1973. The Inhomogeneity of Plastic Deformation. ASM, Metals Park, Ohio, pp. 19–52.
Williams, C.D., Adamson, R.B., Olhausen, K.D., 1974. European Conference on irradiation behavior of fuel cladding and core component materials. Karlsruhe, 189–192.